A multi-wavelenght approach to current blazar issues

Simultaneous *Planck*, *Swift*, and *Fermi* observations of X-ray and γ-ray selected blazars

P. Giommi[2,3], G. Polenta[2,23], A. Lähteenmäki[1,19], D. J. Thompson[5], M. Capalbi[2], S. Cutini[2], D. Gasparrini[2], J. González-Nuevo[43], J. León-Tavares[1], M. López-Caniego[32], M. N. Mazziotta[33], C. Monte[14,33], M. Perri[2], S. Rainò[14,33], G. Tosti[35,15], A. Tramacere[28], F. Verrecchia[2], H. D. Aller[4], M. F. Aller[4], E. Angelakis[41], D. Bastieri[13,34], A. Berdyugin[45], A. Bonaldi[37], L. Bonavera[43,7], C. Burigana[26], D. N. Burrows[10], S. Buson[34], E. Cavazzuti[2], G. Chincarini[46], S. Colafrancesco[23], L. Costamante[47], F. Cuttaia[26], F. D'Ammando[27], G. de Zotti[22,43], M. Frailis[24], L. Fuhrmann[41], S. Galeotta[24], F. Gargano[33], N. Gehrels[5], N. Giglietto[14,33], F. Giordano[14], M. Giroletti[25], E. Keihänen[12], O. King[42], T. P. Krichbaum[41], A. Lasenby[6,38], N. Lavonen[1], C. R. Lawrence[36], C. Leto[2], E. Lindfors[45], N. Mandolesi[26], M. Massardi[22], W. Max-Moerbeck[42], P. F. Michelson[47], M. Mingaliev[44], P. Natoli[16,2,26], I. Nestoras[41], E. Nieppola[1,17], K. Nilsson[17], B. Partridge[18], V. Pavlidou[42], T. J. Pearson[8,29], P. Procopio[26], J. P. Rachen[40], A. Readhead[42], R. Reeves[42], A. Reimer[31,47], R. Reinthal[45], S. Ricciardi[26], J. Richards[42], D. Riquelme[30], J. Saarinen[45], A. Sajina[11], M. Sandri[26], P. Savolainen[1], A. Sievers[30], A. Sillanpää[45], Y. Sotnikova[44], M. Stevenson[42], G. Tagliaferri[21], L. Takalo[45], J. Tammi[1], D. Tavagnacco[24], L. Terenzi[26], L. Toffolatti[9], M. Tornikoski[1], C. Trigilio[20], M. Turunen[1], G. Umana[20], H. Ungerechts[30], F. Villa[26], J. Wu[39], A. Zacchei[24], J. A. Zensus[41], and X. Zhou[39]

A&A 2012, in press ArXiv:1108.1114

- **Large number of sources**:

  175 blazars observed by Swift when they were in the FOV of Planck: **~160 Swift ToOs**

- **Truly simultaneous** Planck Swift Fermi + ground based telescopes

- **Multi-selection approach**. Four flux-limited samples.

  Soft X-ray (RASS, sample)

  Hard X-ray (Swift-BAT sample)

  γ-ray (Fermi sample)

  Radio (100 brightest northern sources)

- Fermi-LAT integrations:

  simultaneous (~1week),

  2 months,

  27 months

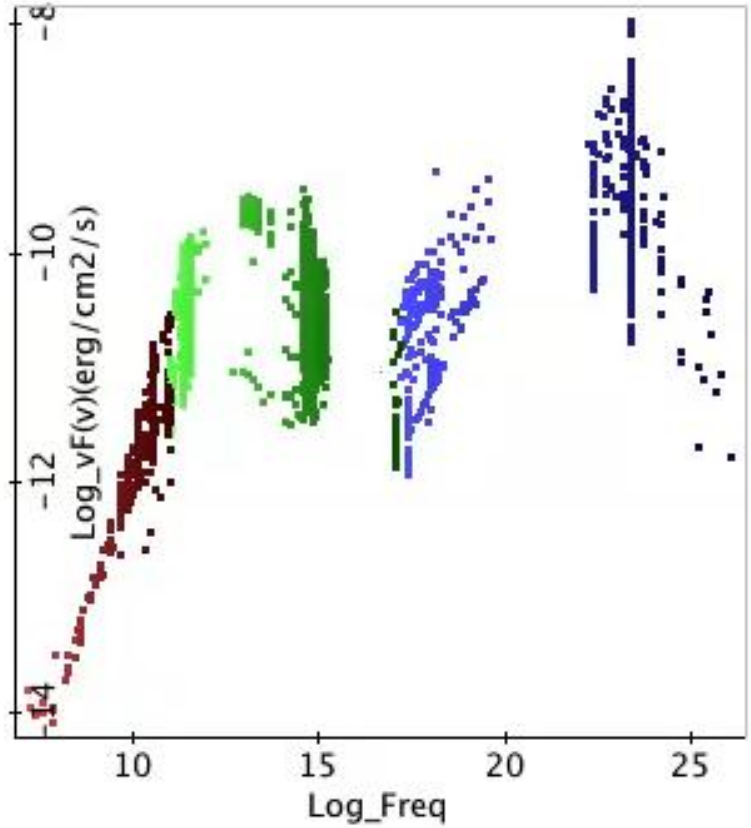
-8
-10
-12
-14
Log_vF(v)(erg/cm2/s)
10
15
20
25
Log_Freq

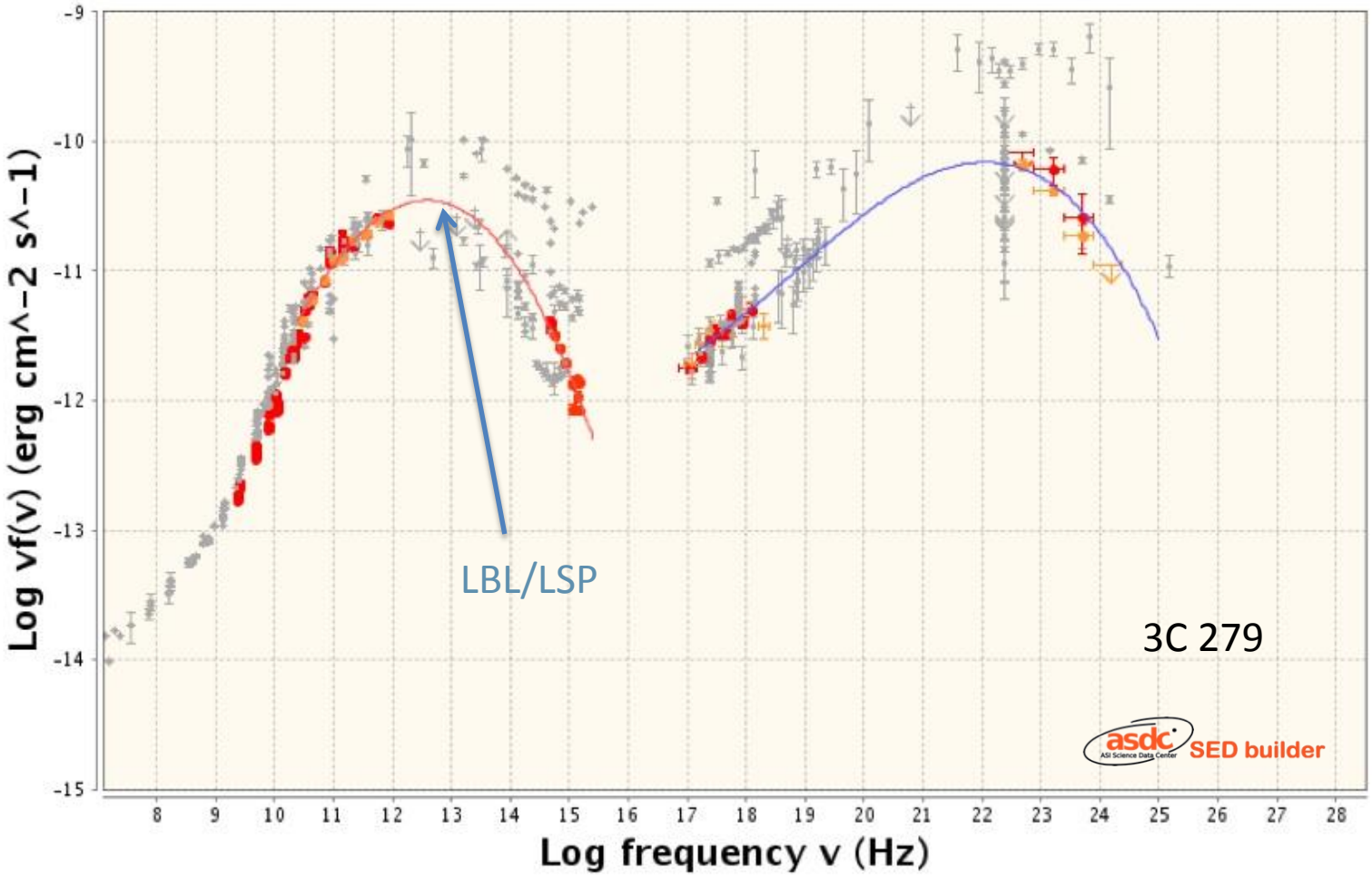
Log vf(v) (erg cm^-2 s^-1)
-9
-10
-11
-12
-13
-14
-15
8
9
10
11
12
13
14
15
16
17
18
19
20
21
22
23
24
25
26
27
28
Log frequency v (Hz)
LBL/LSP
3C 279
asdc SED builder

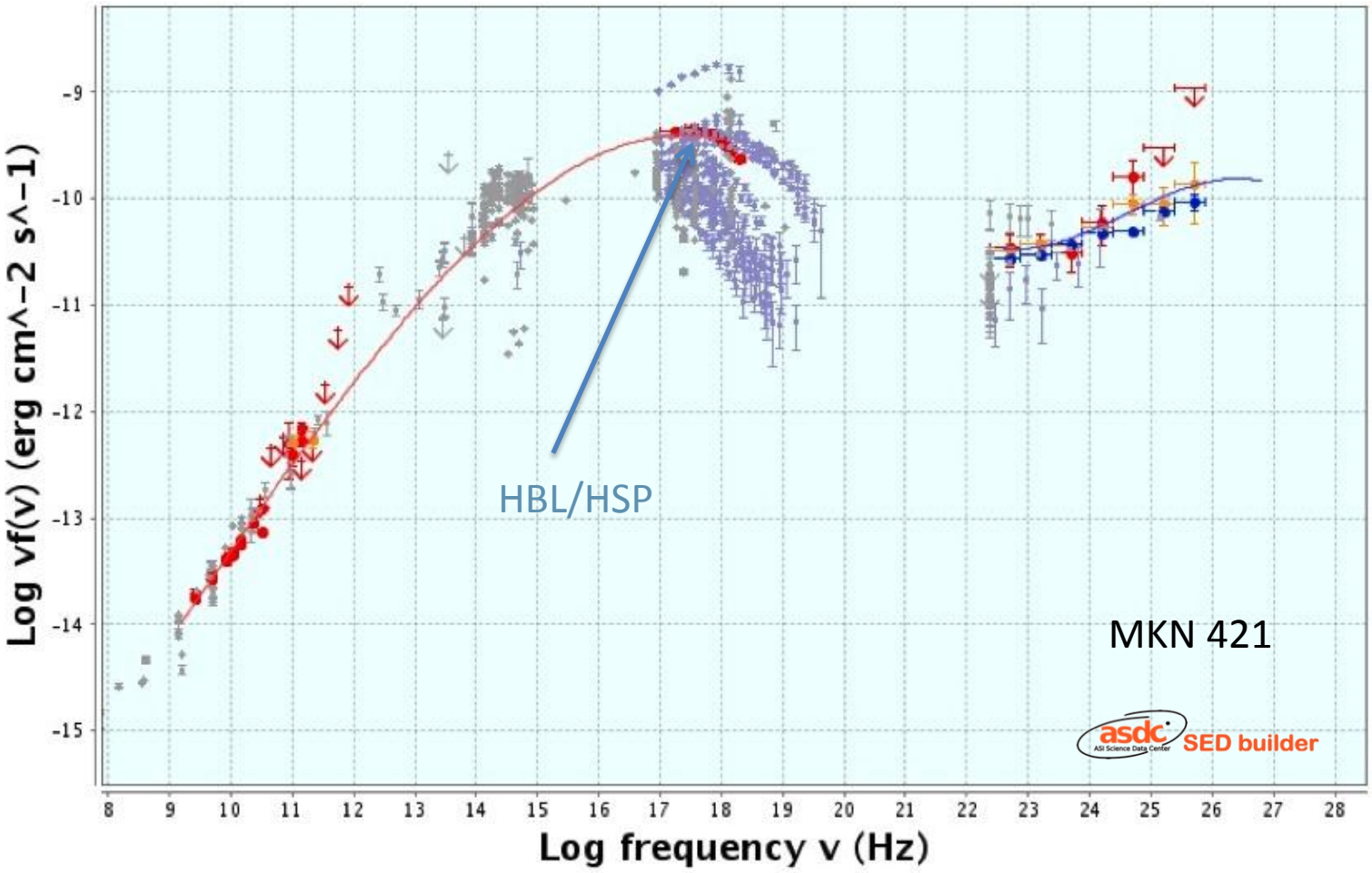
Log vf(v) (erg cm^-2 s^-1)
-9
-10
-11
-12
-13
-14
-15
8
9
10
11
12
13
14
15
16
17
18
19
20
21
22
23
24
25
26
27
28
Log frequency v (Hz)
HBL/HSP
MKN 421
asdc SED builder

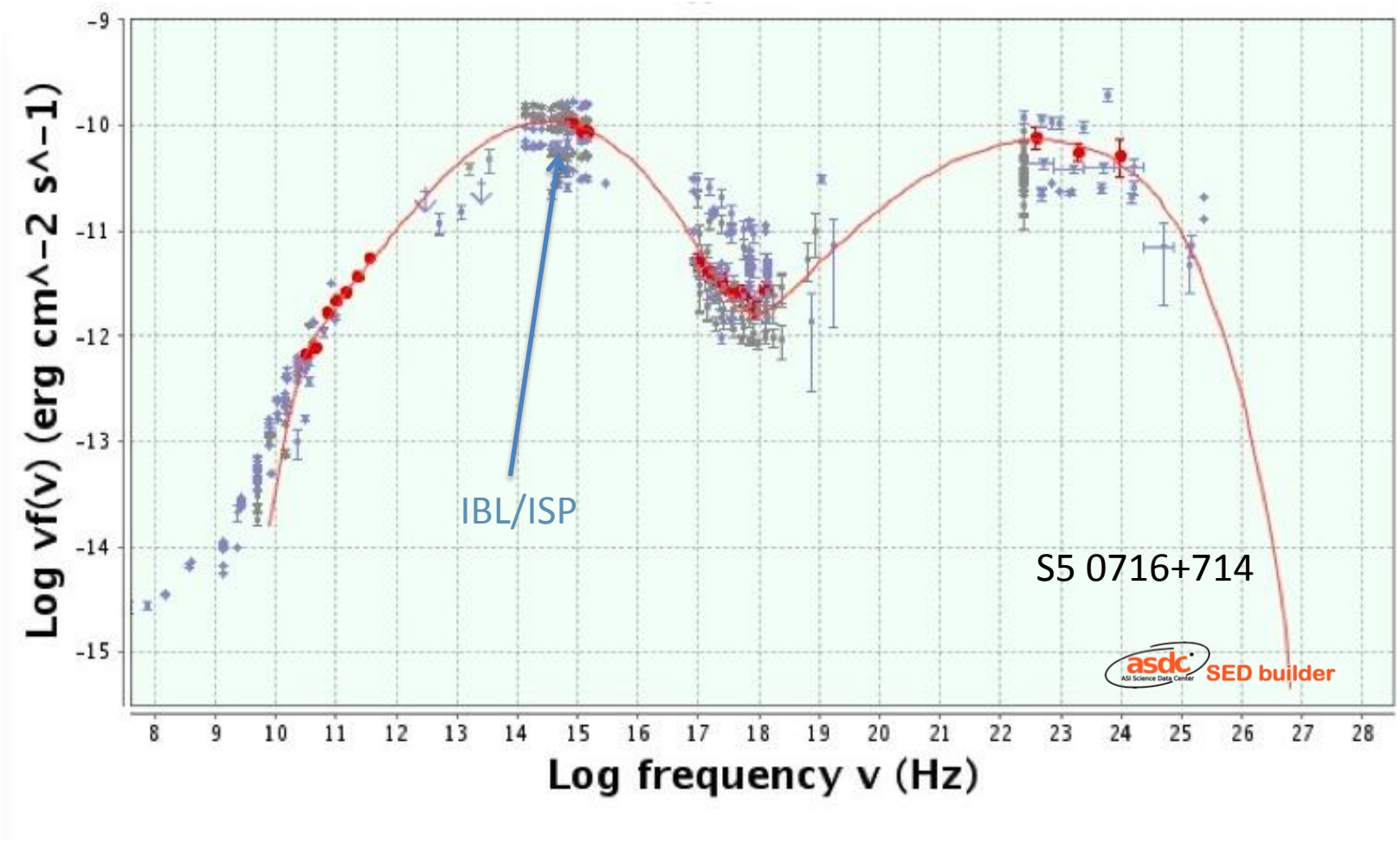
Log vf(v) (erg cm^-2 s^-1)
-9
-10
-11
-12
-13
-14
-15
8
9
10
11
12
13
14
15
16
17
18
19
20
21
22
23
24
25
26
27
28
Log frequency v (Hz)
IBL/ISP
S5 0716+714
asdc SED builder

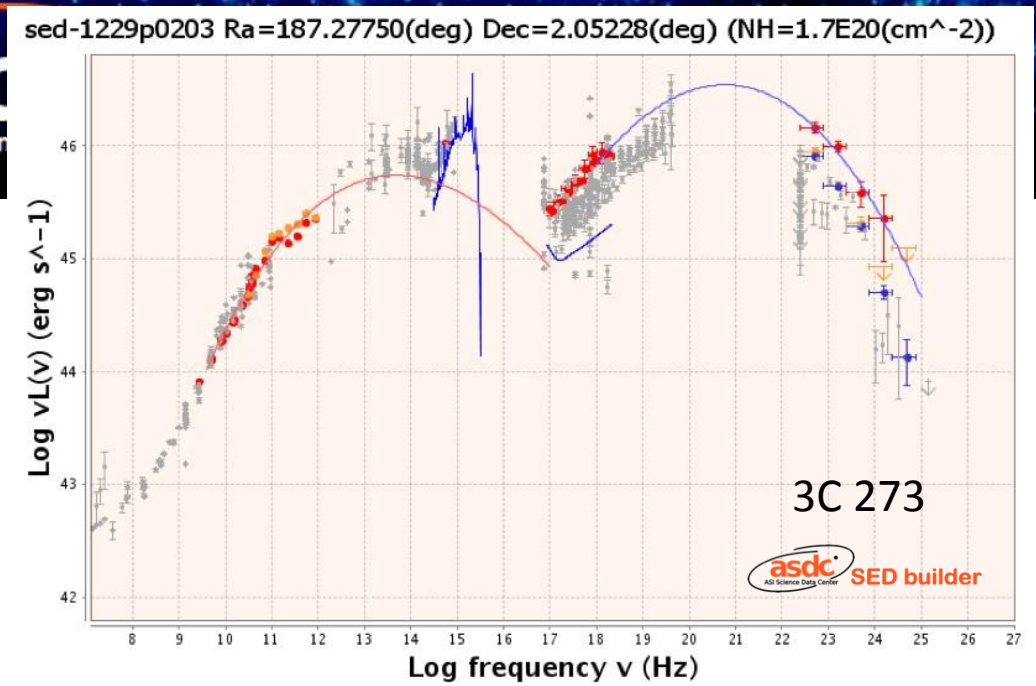
sed-1229p0203 Ra=187.27750(deg) Dec=2.05228(deg) (NH=1.7E20(cm^-2))
Log vL(v) (erg s^-1)
Log frequency v (Hz)
3C 273
asdc SED builder

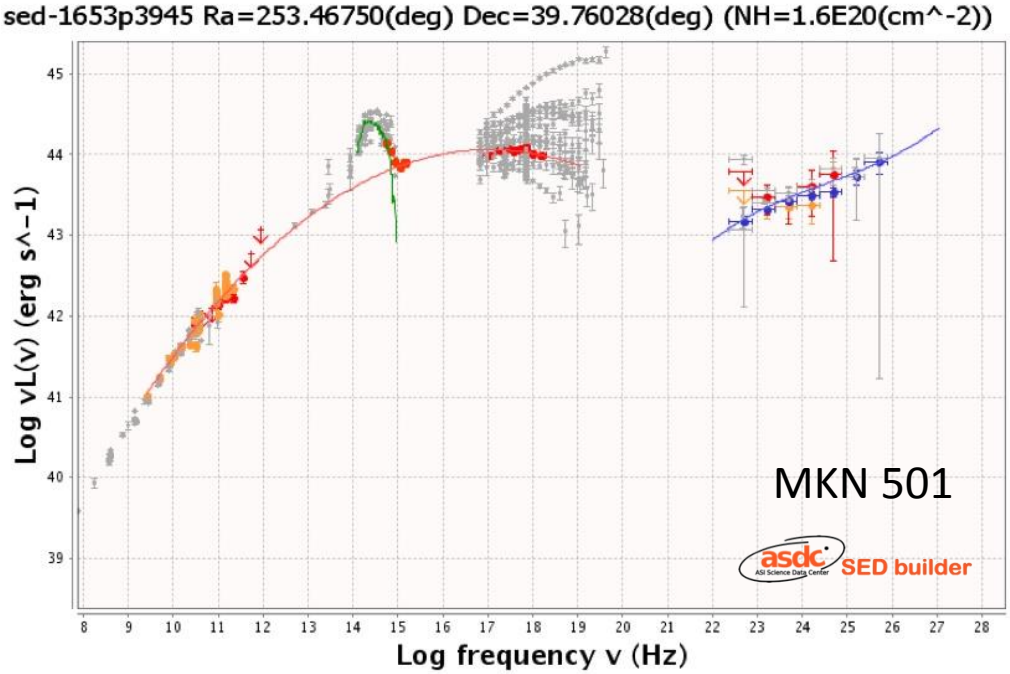
sed-1653p3945 Ra=253.46750(deg) Dec=39.76028(deg) (NH=1.6E20(cm^-2))
Log vL(v) (erg s^-1)
Log frequency v (Hz)
MKN 501
asdc SED builder

Summary of γ-ray detections (TS > 25) in 27 month Fermi-LAT data.

Sample	No. of detected sources		
	FSRQs	BL Lacs	Uncertain
Fermi-LAT	28 (100%)	14 (100%)	8 (100%)
Swift-BAT	17 (63%)	7 (100%)	3 (50%)
Rosat/RASS	8 (53%)	14 (88%)	2 (17%)
Radio	43 (72%)	16 (100%)	9 (64%)

The synchrotron/invC peak frequencies ν_{peak} and intensities ν_{peak} $f(\nu_{peak})$

Measured using 3rd degree polynomial functions

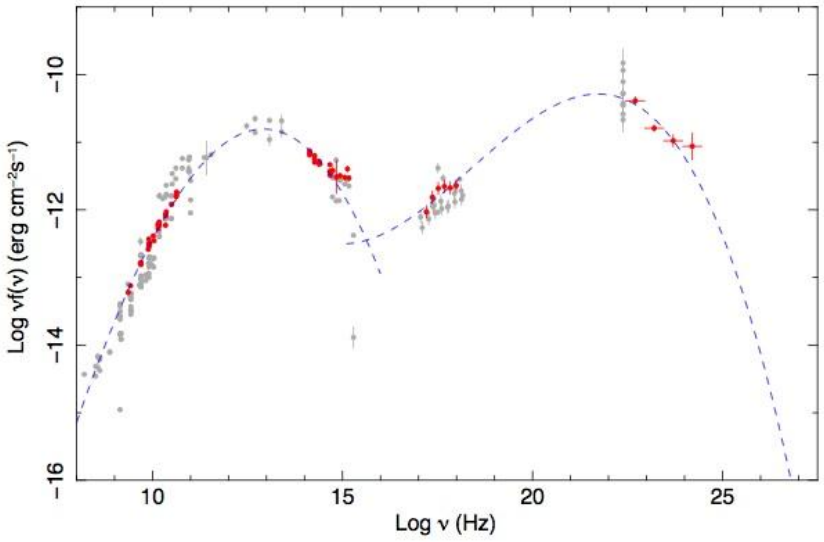

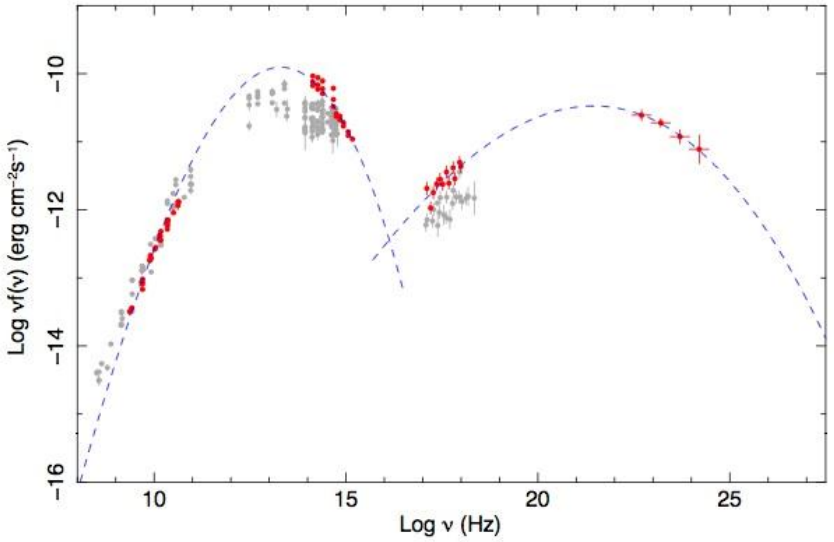

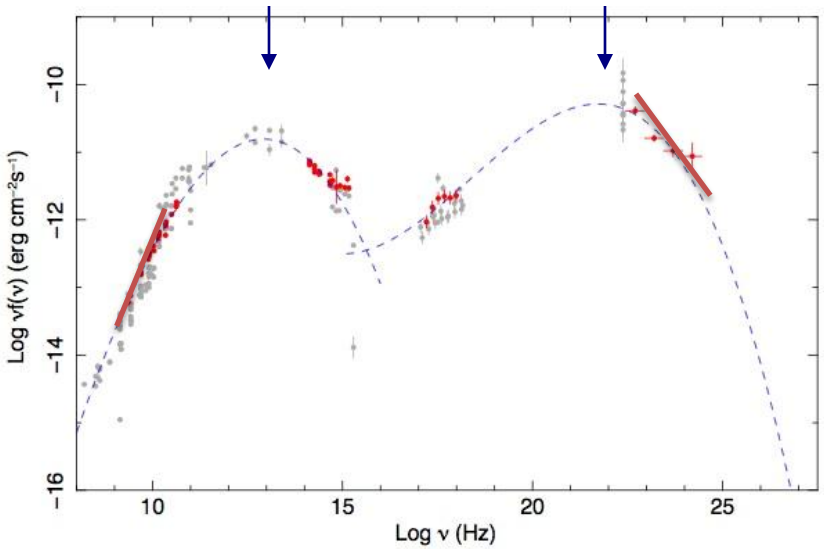
Log νf(ν) (erg cm⁻²s⁻¹)
−10
−12
−14
−16
10
15
20
25
Log ν (Hz)

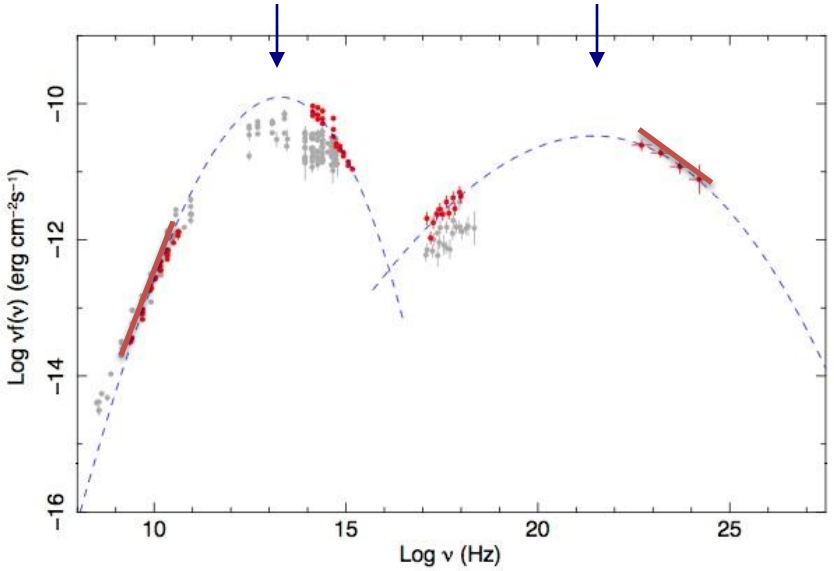
Log νf(ν) (erg cm⁻²s⁻¹)
−10
−12
−14
−16
10
15
20
25
Log ν (Hz)

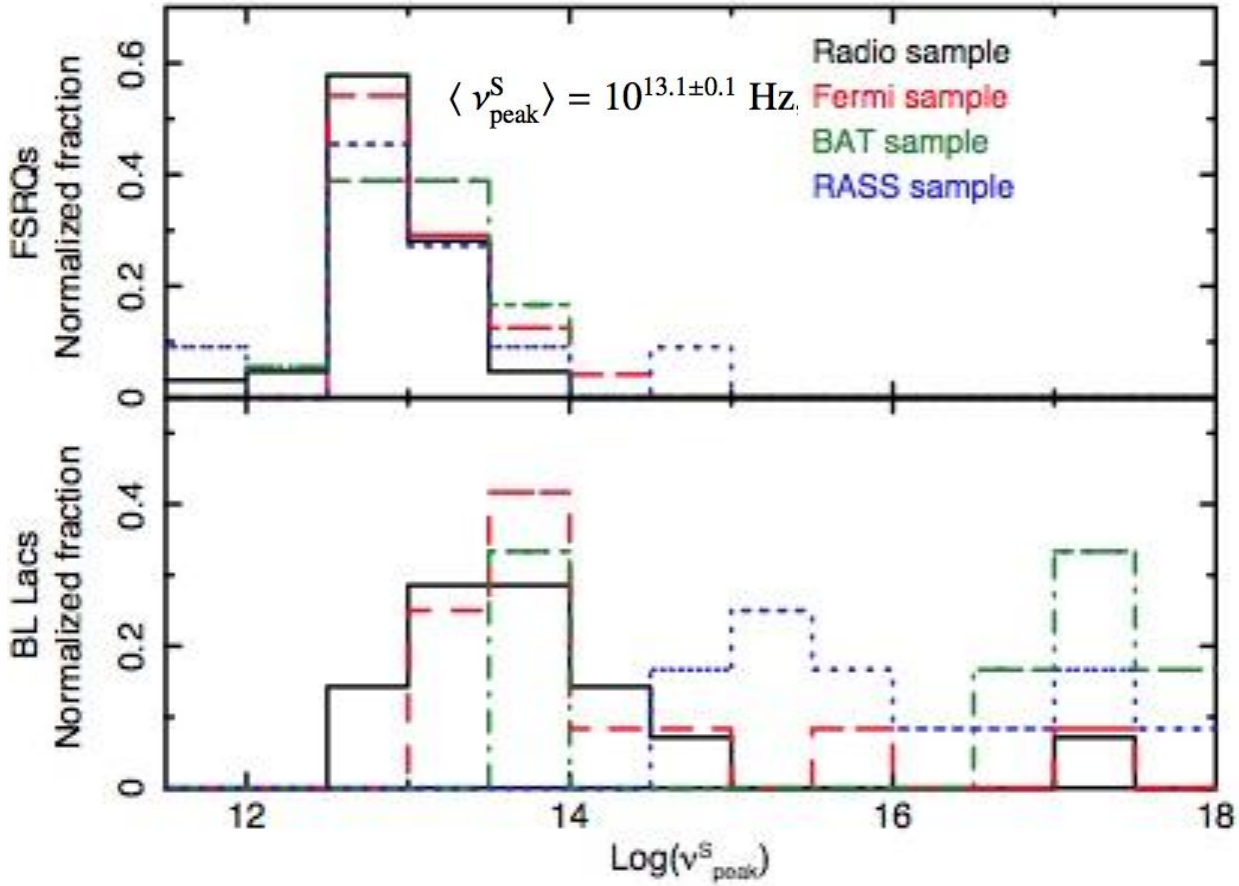
$\langle \nu^S_{peak} \rangle = 10^{13.1\pm0.1}$ Hz
Radio sample
Fermi sample
BAT sample
RASS sample
FSRQs
Normalized fraction
BL Lacs
Normalized fraction
0
0.2
0.4
0.6
12
14
16
18
Log(ν^S_{peak})

The Compton dominance

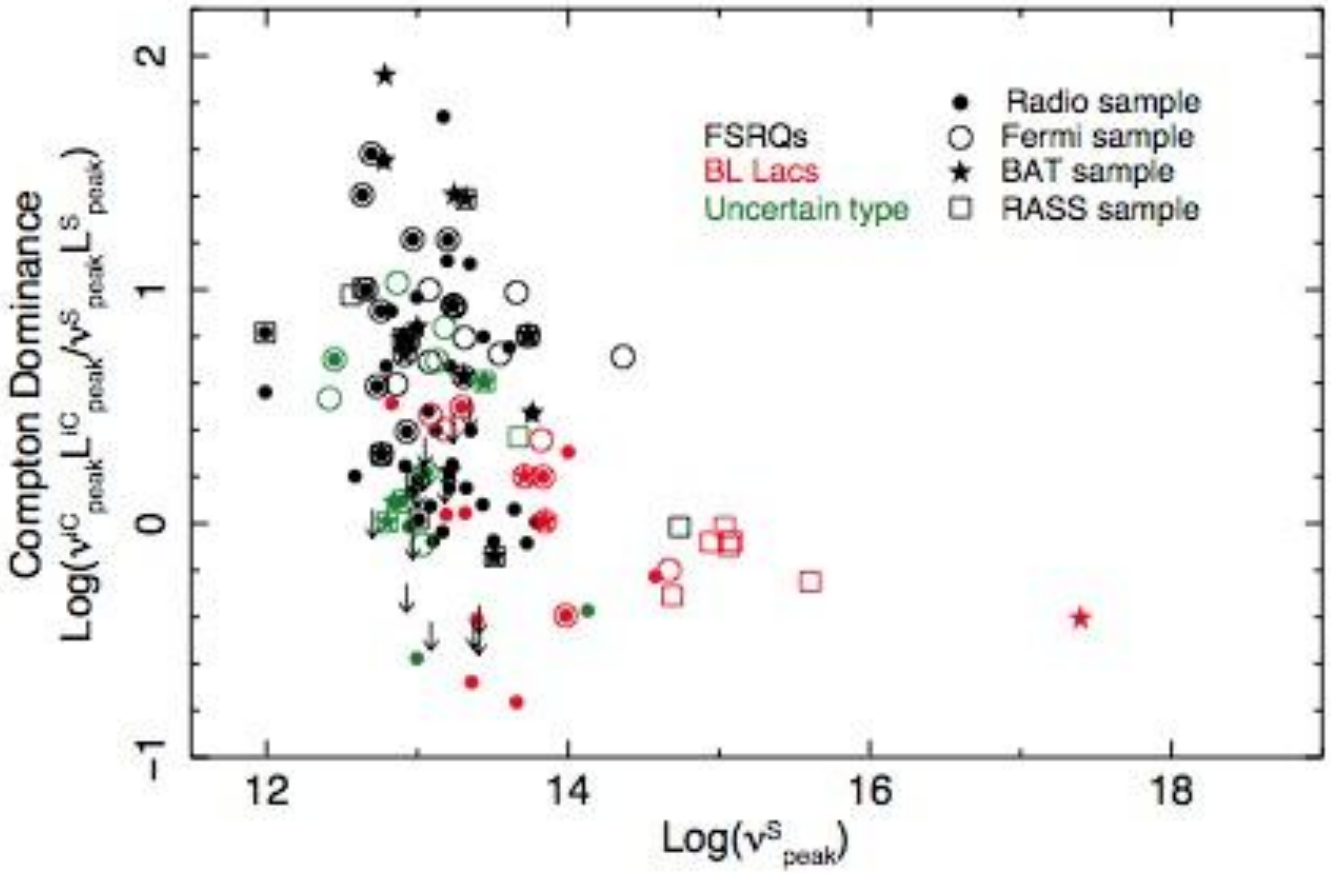

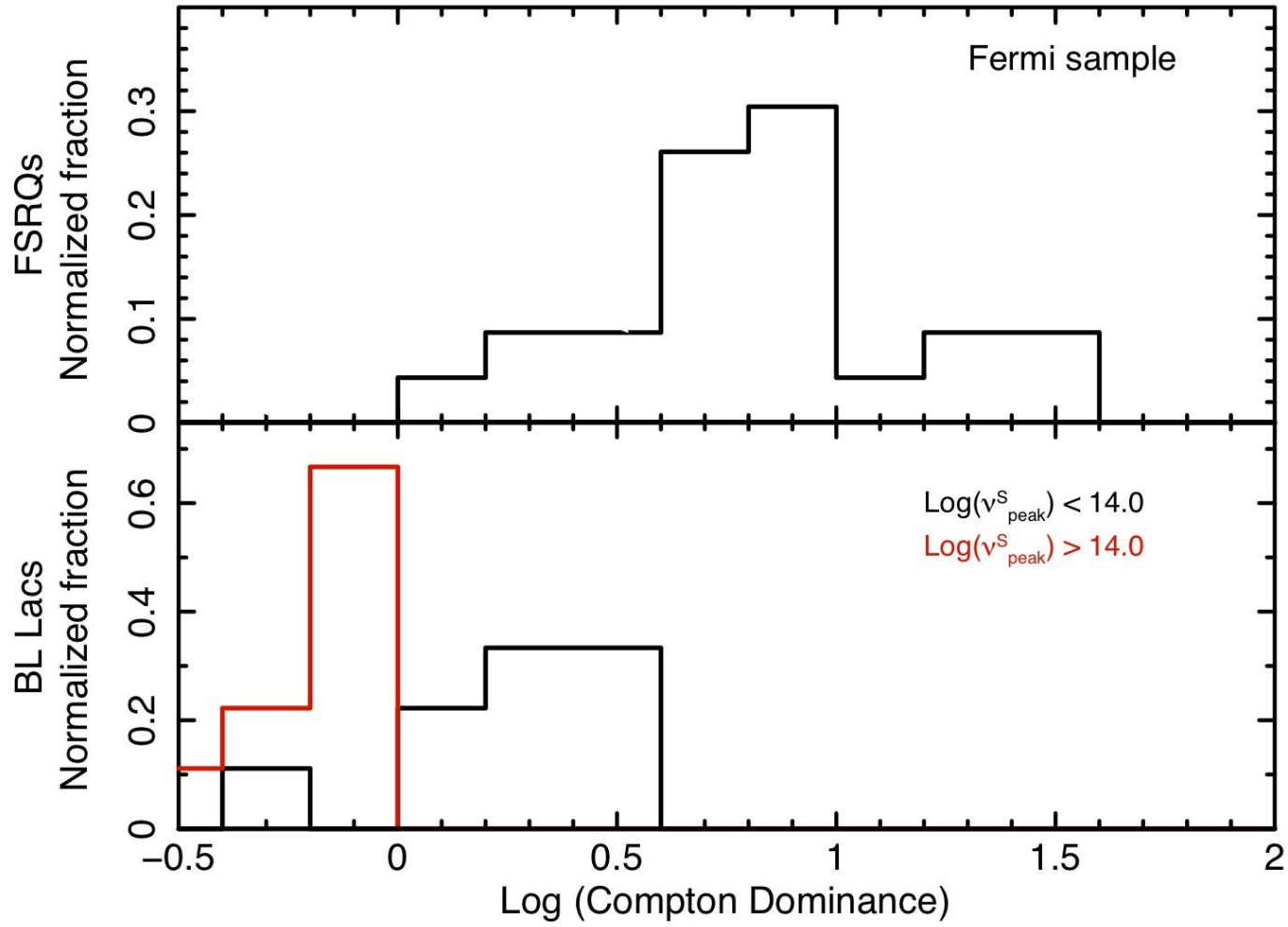
Fermi sample
FSRQs
Normalized fraction
0
0.1
0.2
0.3
BL Lacs
Normalized fraction
0
0.2
0.4
0.6
Log(ν^S_peak) < 14.0
Log(ν^S_peak) > 14.0
–0.5
0
0.5
1
1.5
2
Log (Compton Dominance)

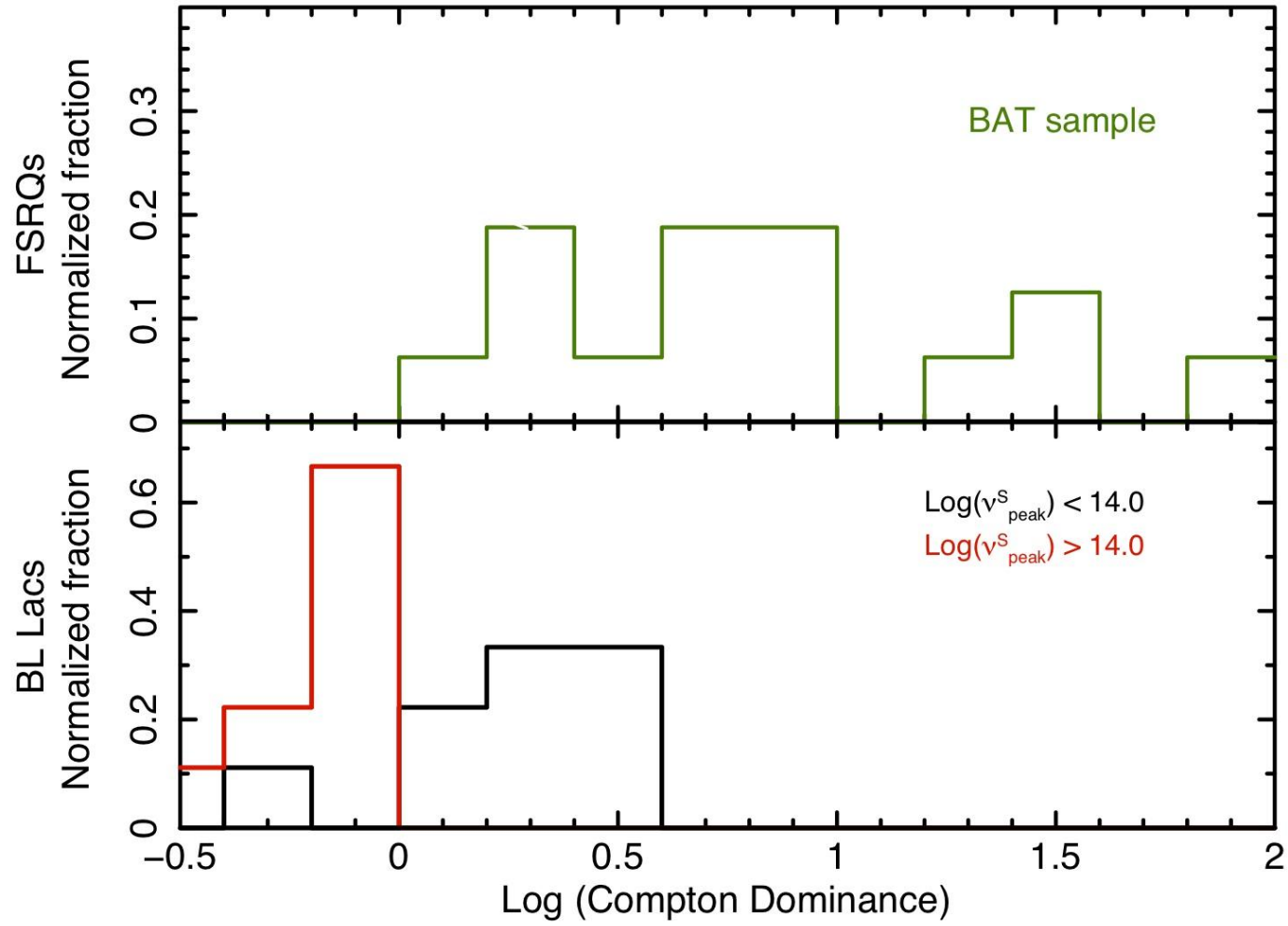
FSRQs
Normalized fraction
BAT sample
BL Lacs
Normalized fraction
Log(ν^{S}_{peak}) < 14.0
Log(ν^{S}_{peak}) > 14.0
0
0.1
0.2
0.3
0.4
0.6
−0.5
0
0.5
1
1.5
2
Log (Compton Dominance)

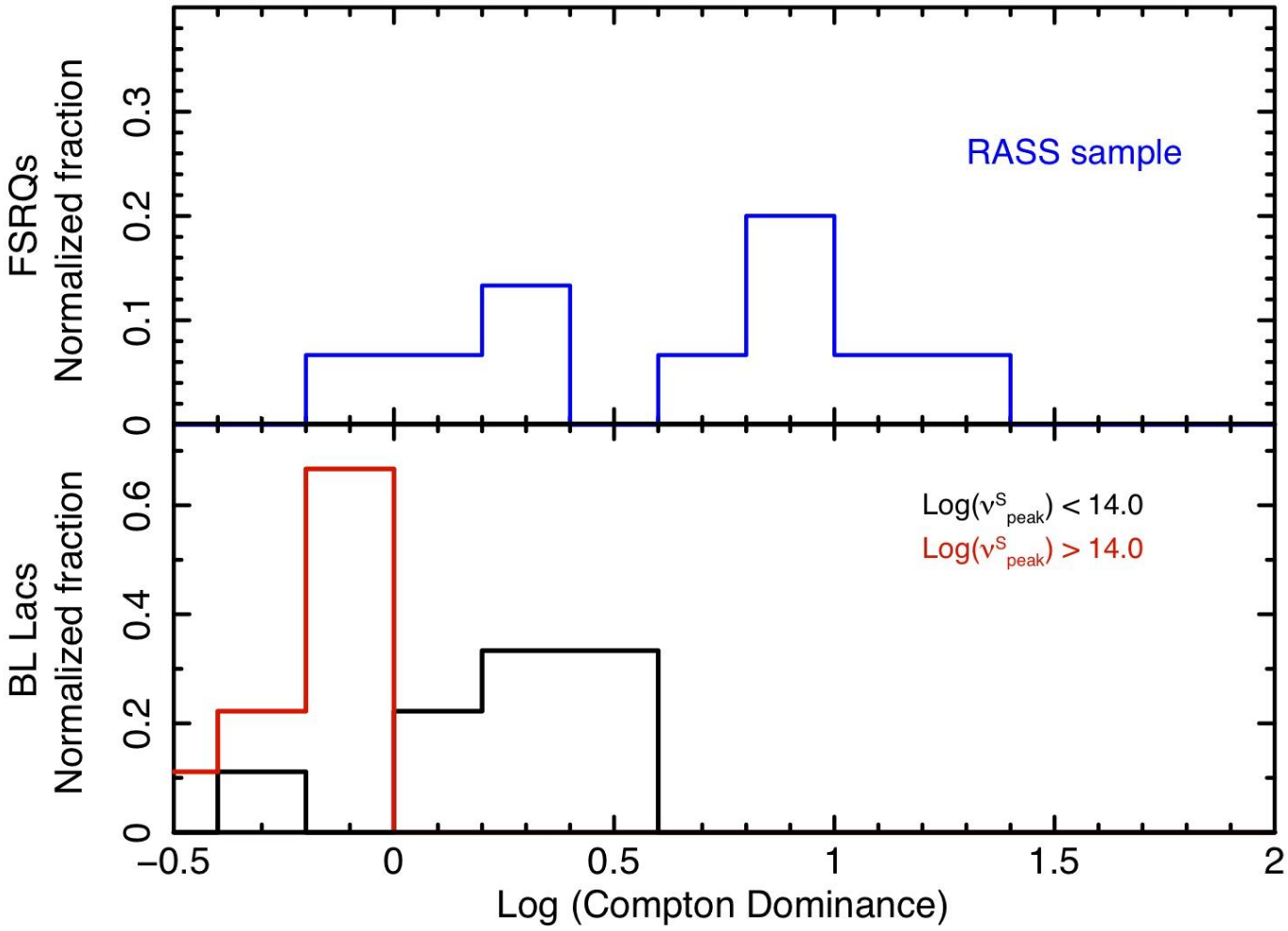
FSRQs
Normalized fraction
0
0.1
0.2
0.3
RASS sample
BL Lacs
Normalized fraction
0
0.2
0.4
0.6
Log(ν^S_peak) < 14.0
Log(ν^S_peak) > 14.0
−0.5
0
0.5
1
1.5
2
Log (Compton Dominance)

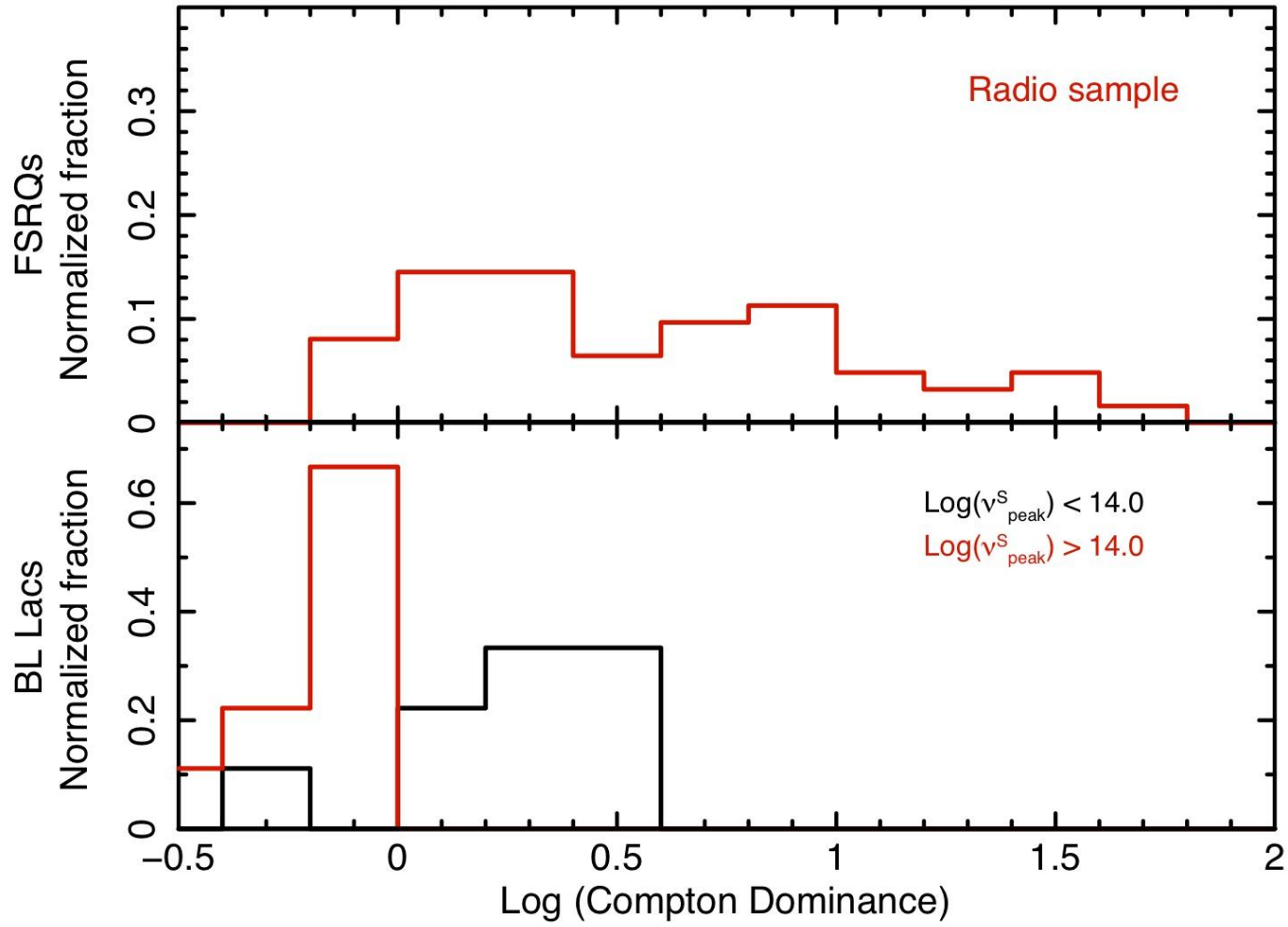
Radio sample
FSRQs
Normalized fraction
0
0.1
0.2
0.3
BL Lacs
Normalized fraction
0
0.2
0.4
0.6
Log(ν^S_peak) < 14.0
Log(ν^S_peak) > 14.0
–0.5
0
0.5
1
1.5
2
Log (Compton Dominance)

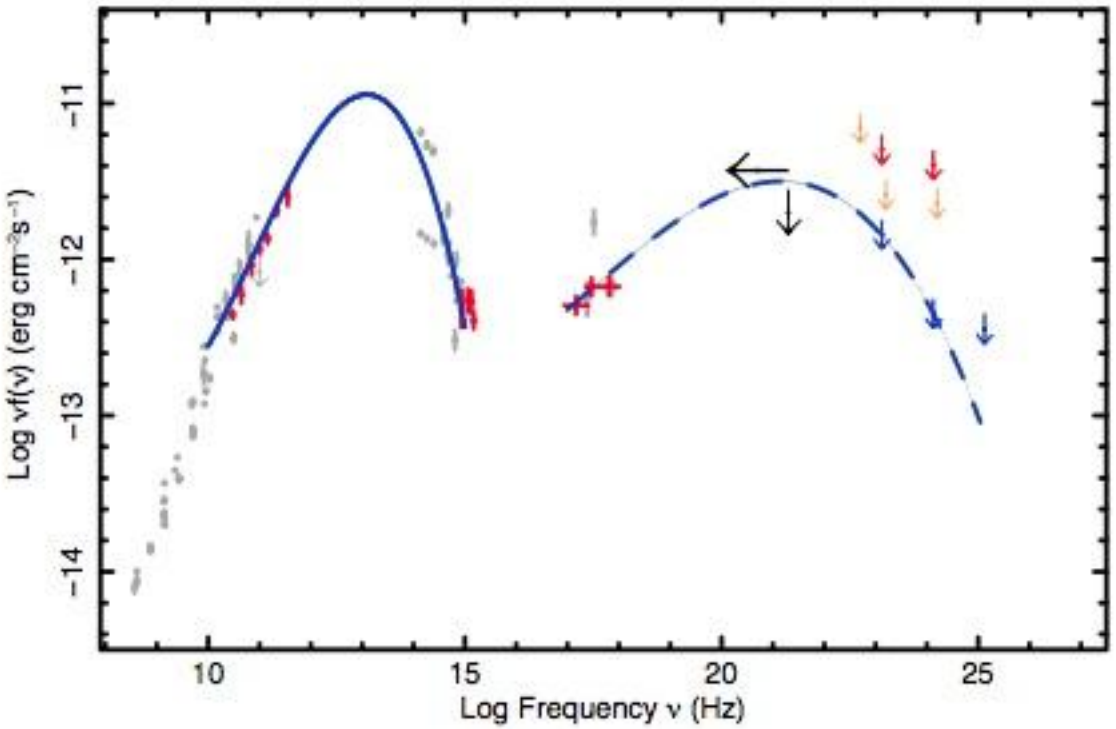

Fig. 10. The SED of the blazar PKS0003-066 as an example of estimation of the upper limits on ν^{IC}_{peak} and on $\nu^{IC}_{peak} F(\nu^{IC}_{peak})$ combining the X-ray data with the 27 month *Fermi*-LAT upper limits.

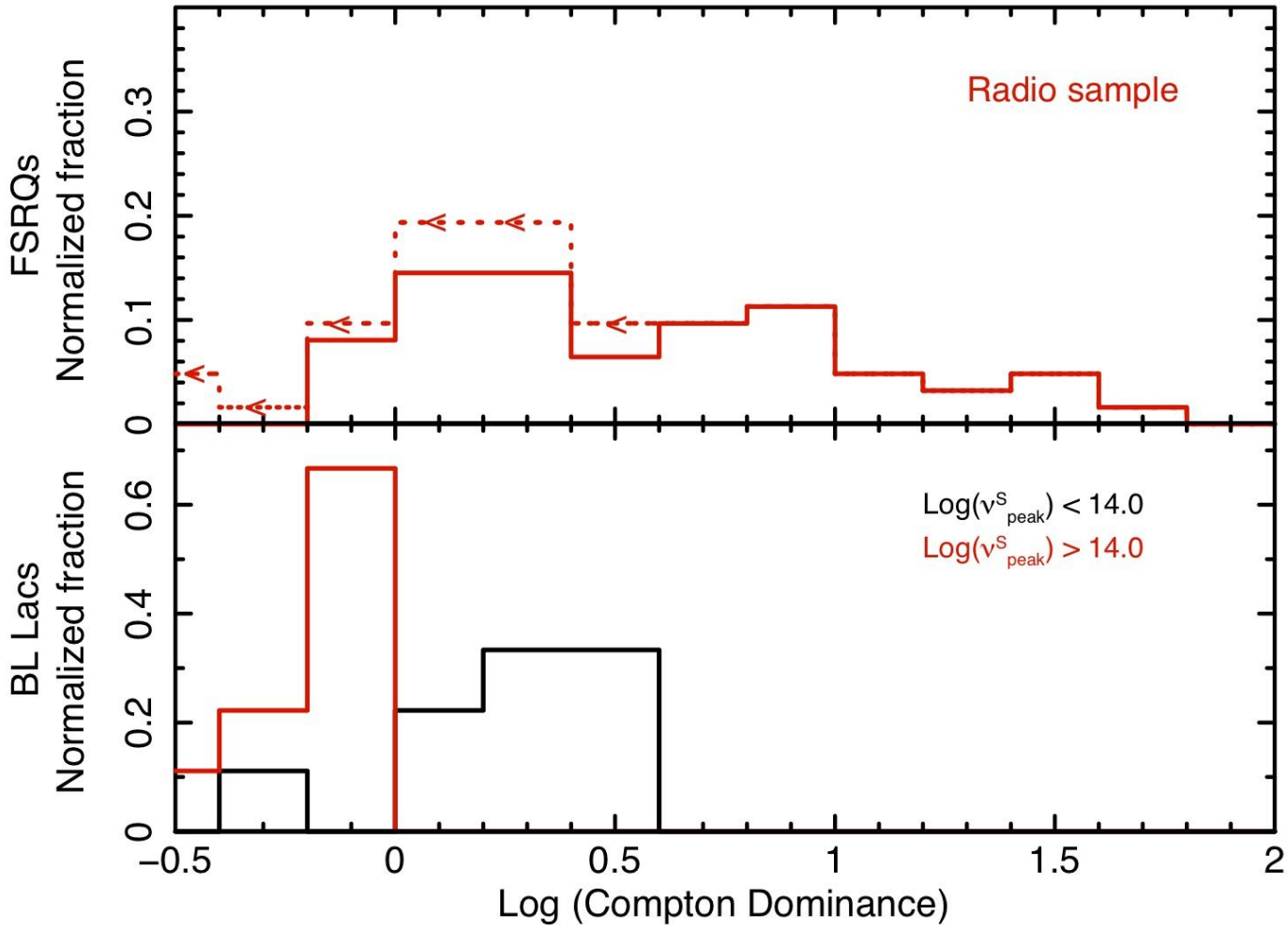
Radio sample
FSRQs
Normalized fraction
0
0.1
0.2
0.3
BL Lacs
Normalized fraction
0
0.2
0.4
0.6
Log(ν^S_peak) < 14.0
Log(ν^S_peak) > 14.0
−0.5
0
0.5
1
1.5
2
Log (Compton Dominance)

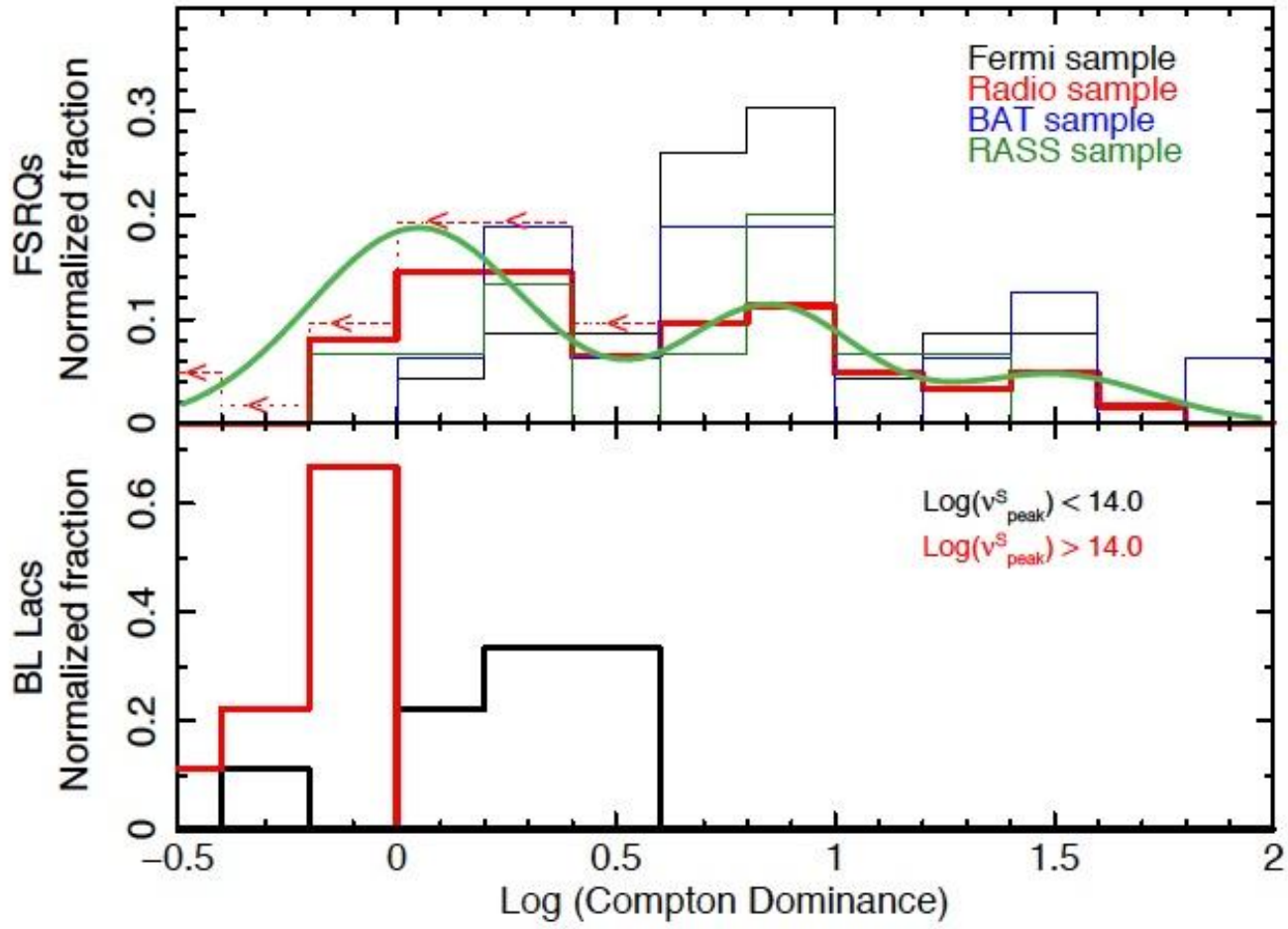

Most (radio selected) FSRQs have Compton Dominance ~ 1 (Log(CD) = 0)

A simplified view of blazars: clearing the fog around long-standing selection effects

P. Giommi[1⋆], P. Padovani[2], G. Polenta[1,3], S. Turriziani[1], V. D'Elia[1,3], S. Piranomonte[3]

[1] *ASI Science Data Center, c/o ESRIN, via G. Galilei, 00044 Frascati, Italy*
[2] *European Southern Observatory, Karl-Schwarzschild-Str. 2, D-85748 Garching bei München, Germany*
[3] *INAF-Osservatorio Astronomico di Roma, via Frascati 33, I-00040 Monteporzio Catone, Italy*

MNRAS, 2012, 420, 2899

Based on

- **beaming (of FR I + FR II radio galaxies, unified schemes)**
- **light dilution (non-thermal jet + accretion + host galaxy)**
- **minimal physical assumptions for the non-thermal/jet emission**

Monte Carlo Simulations: The ingredients

- Luminosity function + Evolution estimated from WMAP blazars
- Unified schemes
- Non-thermal component: SSC with single distribution of electron peak energies and Doppler factors. No dependence on luminosity or redshift
- Thermal component + broad lines from SDSS template
- EW distribution from radio quiet QSOs (estimated from SDSS spectra)
- Disk to jet power ratio estimated from the SED a large number of blazars
- Host Galaxy: Giant elliptical

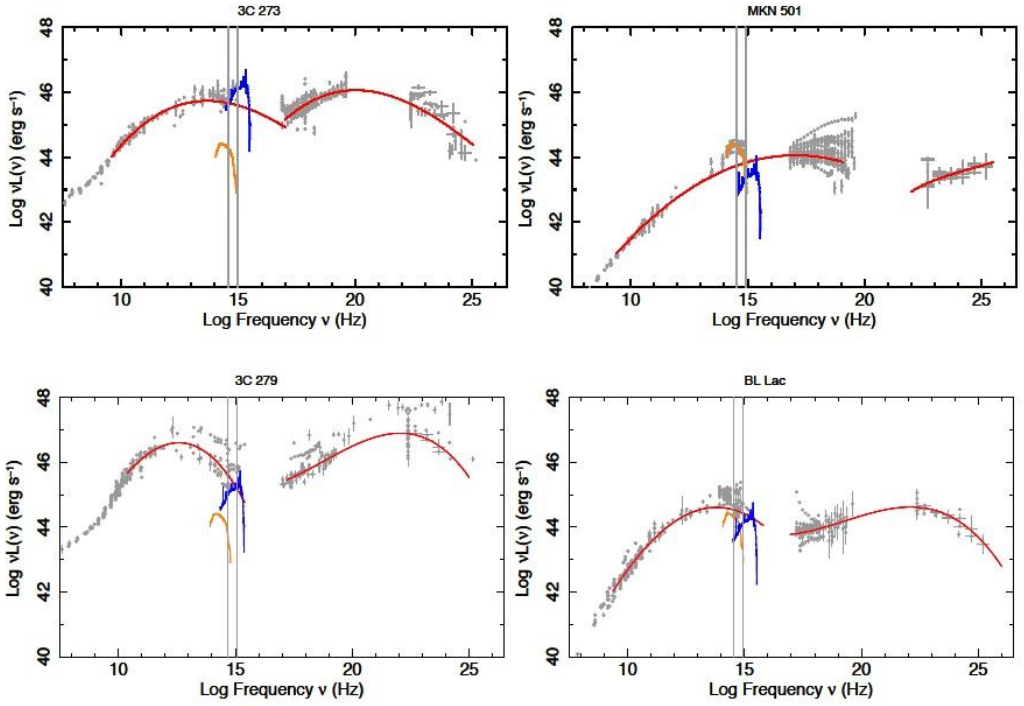

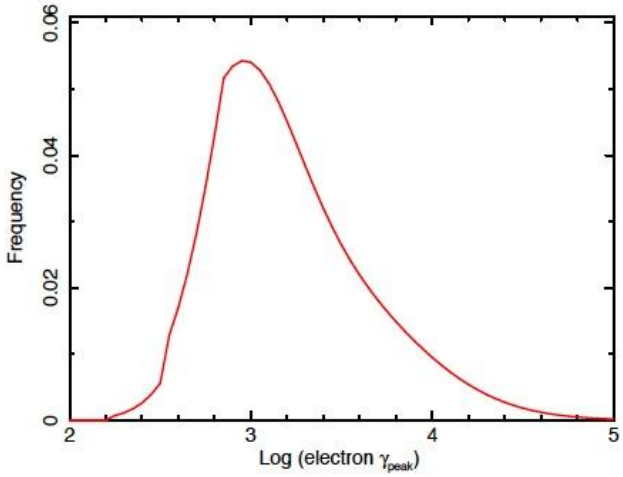

Figure 4. The distribution of the Lorentz factors of the electrons radiating at the peak of the synchrotron SED used for the simulation, which also assumes a magnetic field of B=0.15 Gauss and a gaussian distribution of Doppler factors with $\langle\delta\rangle$=15.

Blazar classification

A simulated source is classified as FSRQ, BL Lac or radio galaxy on the basis of the balance of Thermal, Blue-bump/broad-lines, non-thermal/jet radiation and host galaxy in the optical band (3800-8000 Å in the observer frame)

- **FSRQ** if the rest-frame EW (Non-thermal + Blue bump) of any line in the optical band is > 5 Å
- **BL-Lac** if the observed EW (Non-thermal + Blue bump) of any line in the optical band (observer frame) is < 5 Å
- **Radio Galaxy** if only absorption features form the host galaxy are in the optiacal band and Ca H&K break > 0.4

Redshift of BL Lacs is assumed to be ***not measurable*** if the EW of the brightest line in the optical band is < 2 Å

	FR I/LERGs	FR II/HERGs	Viewing angle
Strong jet dilution (ew < 5 Å, CaH&K < 0.4)	BL Lac	*BL Lac*	$\Theta < \theta_{blazar}$
Weak jet dilution	*Radio galaxy*	FSRQ	$\Theta < \theta_{blazar}$
Misdirected Jet	Radio galaxy	Radio galaxy	$\Theta > \theta_{blazar}$

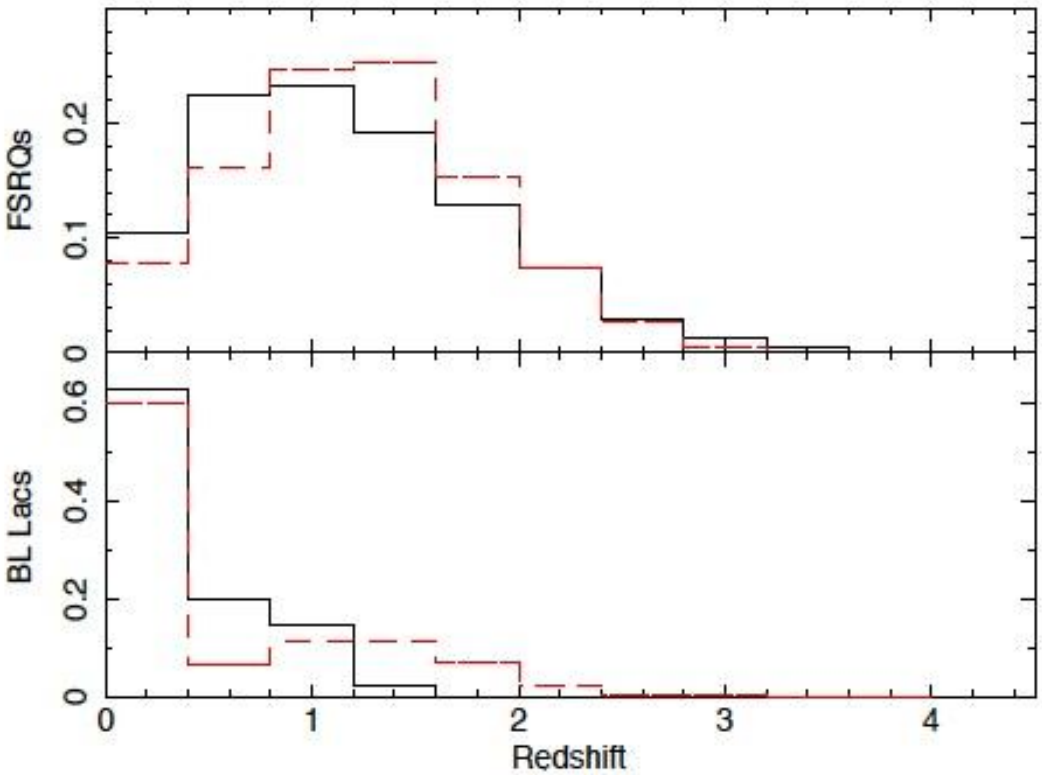

Figure 6. Top panel: the redshift distribution of the WMAP5 FSRQs (solid histogram) compared to that of FSRQs in a simulation of a radio survey (dashed histogram). Bottom panel: the redshift distribution of the WMAP5 BL Lacs (solid histogram) compared to that of BL Lacs in a simulation of a radio survey (dashed histogram)

Results

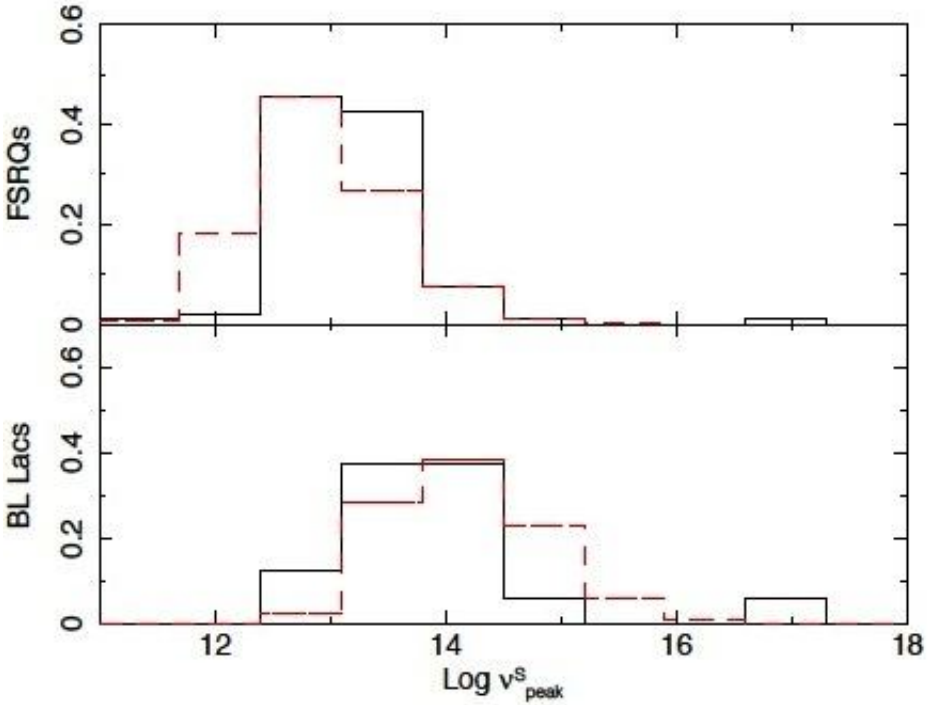

Figure 8. Top panel: the $\nu^S_{\rm peak}$ distribution of radio selected FSRQs taken from the work of Giommi et al. (2011) (solid histogram) compared to that of FSRQs in a simulation of a

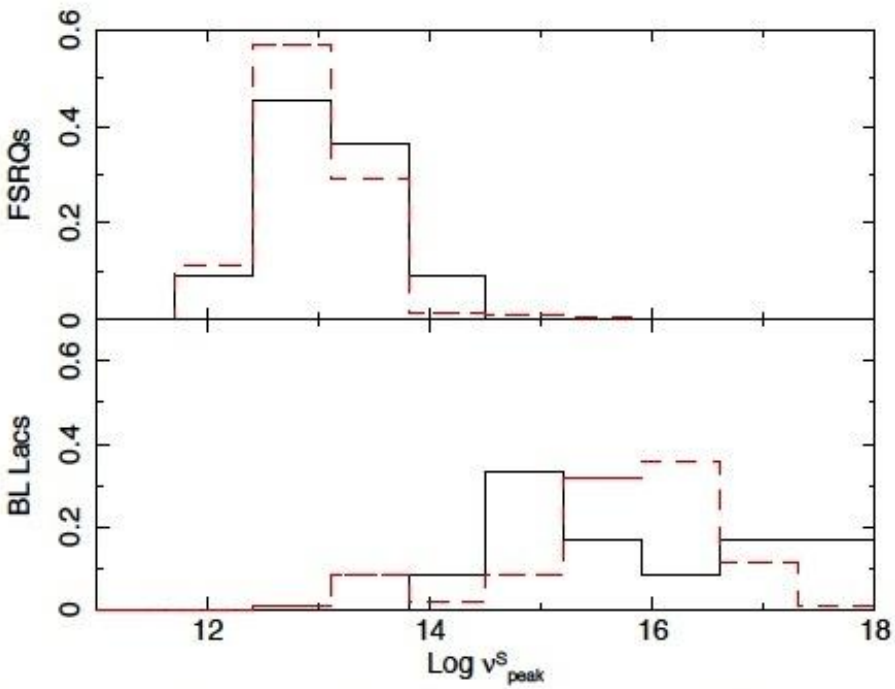

Figure 10. Top panel: the $\nu^S_{\rm peak}$ distribution of the X-ray selected FSRQs in Giommi et al. (2011) (solid histogram) compared to that of FSRQs in a simulation of an X-ray survey

The different synchrotron peak energy distributions in BL Lacs and FSRQs is NOT due to cooling or other physical reason, but to selection effects!

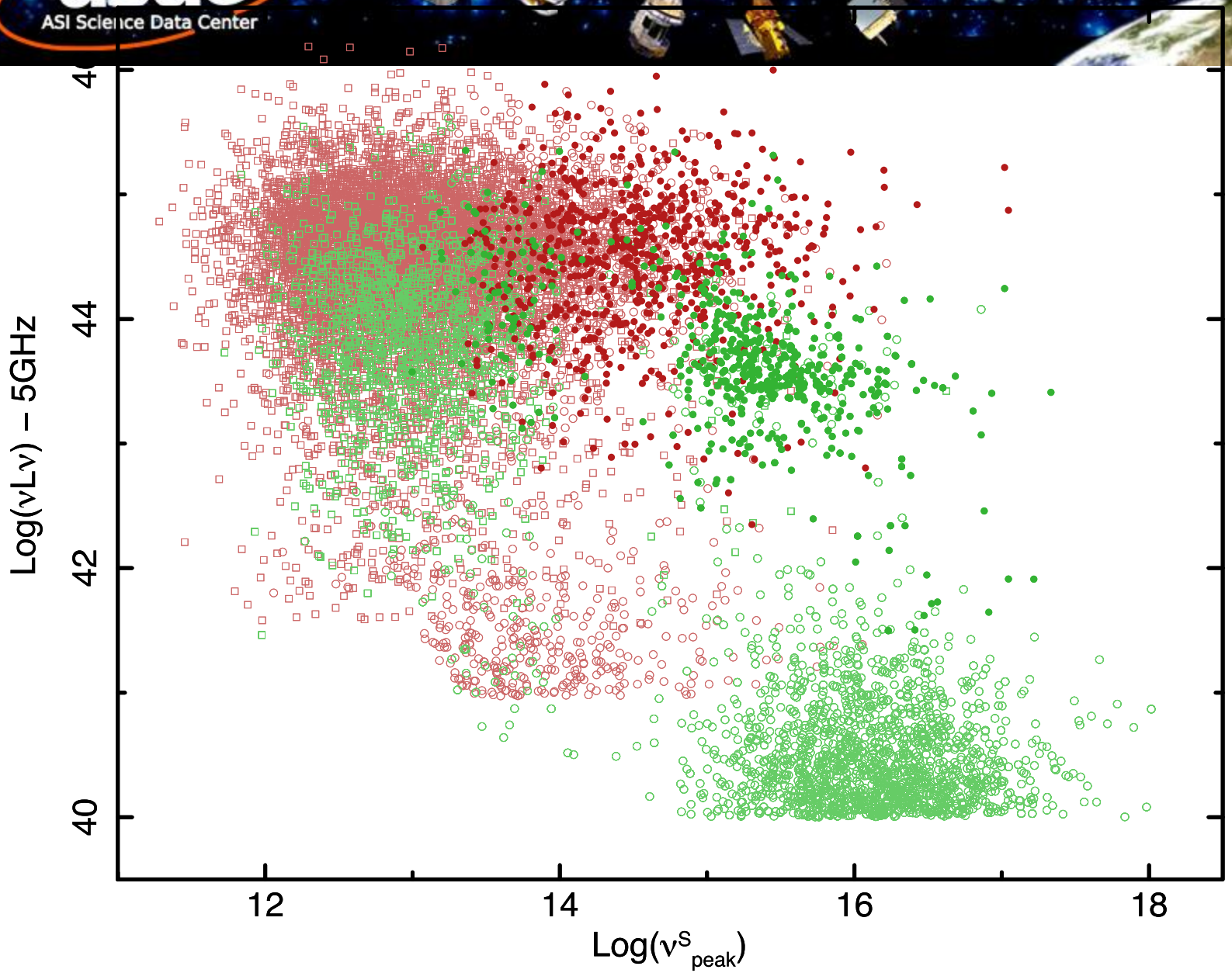
Log(νLν) – 5GHz
40
42
44
12
14
16
18
Log(ν^S_peak)

BL Lacertae objects beyond redshift 1.3 - UV-to-NIR photometry and photometric redshift for Fermi/LAT blazars

A. Rau,[1], P. Schady,[1], J. Greiner[1], M. Salvato[2,3], M. Ajello[4,5], E. Bottacini[4], N. Gehrels[6], P. M. J. Afonso[1,7], J. Elliott[1], R. Filgas[1], D. A. Kann[8], S. Klose[8], T. Krühler[1,3,9], M. Nardini[1,10], A. Nicuesa Guelbenzu[8], F. Olivares E.[1], A. Rossi[8], V. Sudilovsky[1], A. C. Updike[11], and D. H. Hartmann[12]

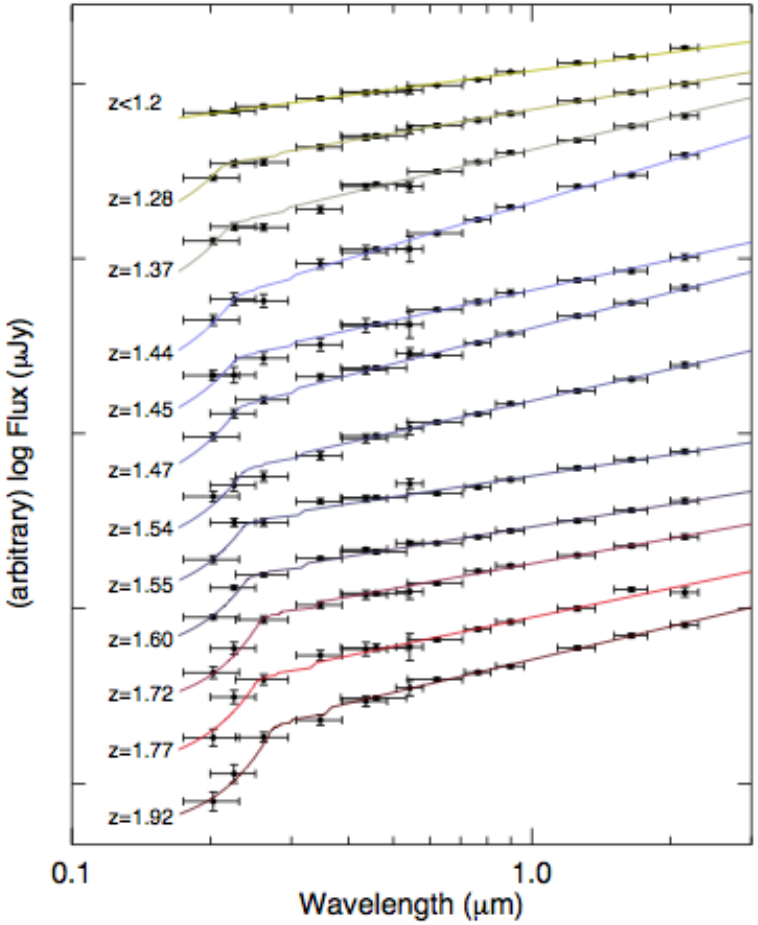

A&A 2012, 538, 26, arXiv1112.0025

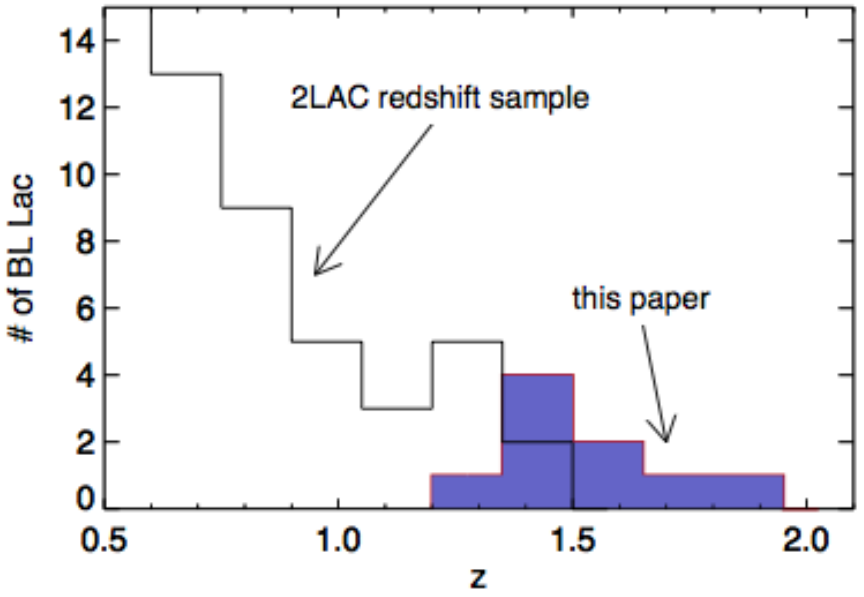

The discovery of high power – high synchrotron peak blazars

MNRAS, in press,arXiv:1202.2236

P. Padovani[1⋆], P. Giommi[2], and A. Rau[3]
[1]*European Southern Observatory, Karl-Schwarzschild-Str. 2, D-85748 Garching bei München, Germany*
[2]*ASI Science Data Center, c/o ESRIN, via G. Galilei, I-00044 Frascati, Italy*
[3]*Max-Planck-Institut für Extraterrestrische Physik, Giessenbachstr. 1, D-85748 Garching bei München, Germany*

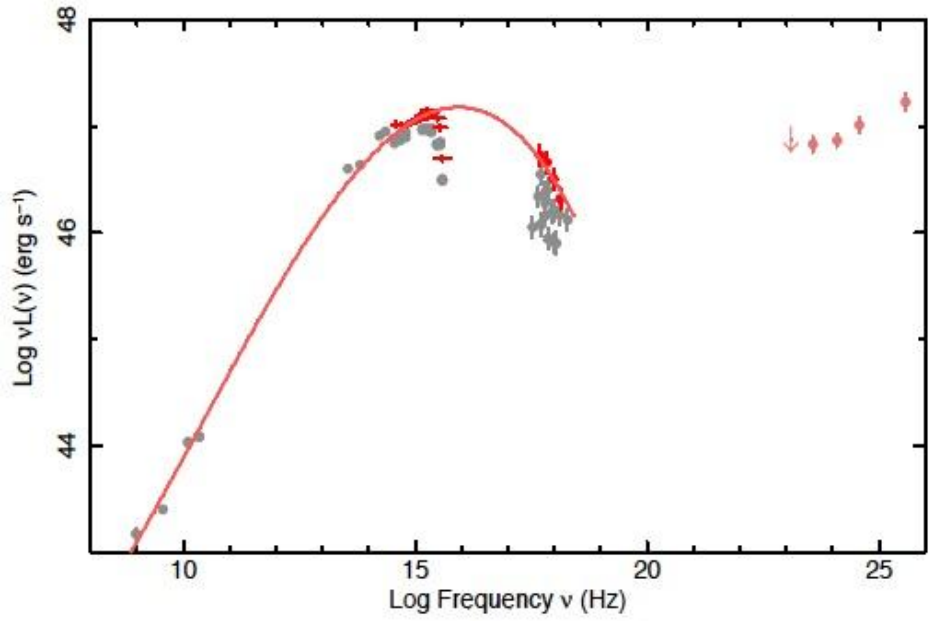

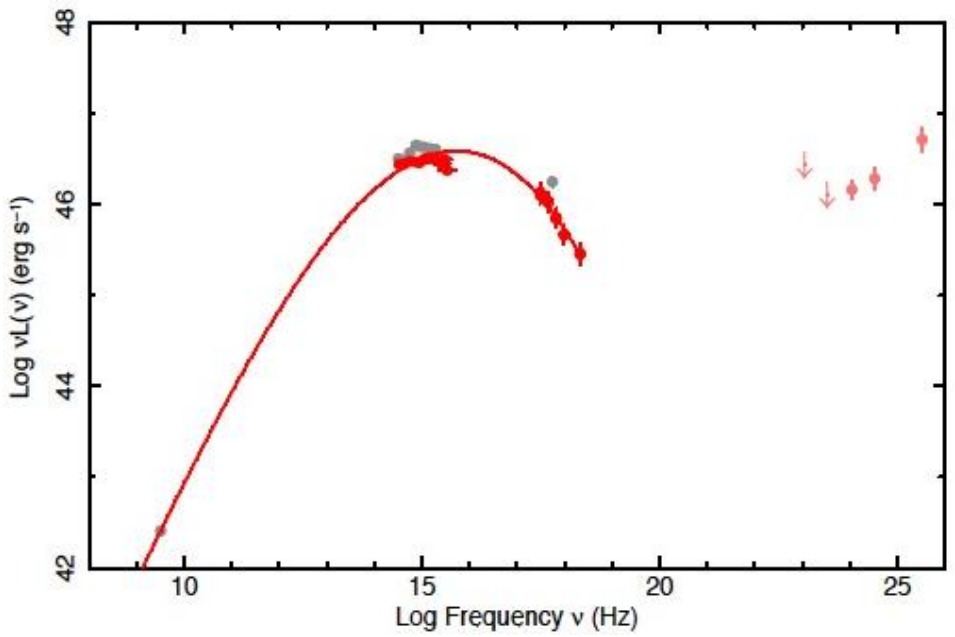

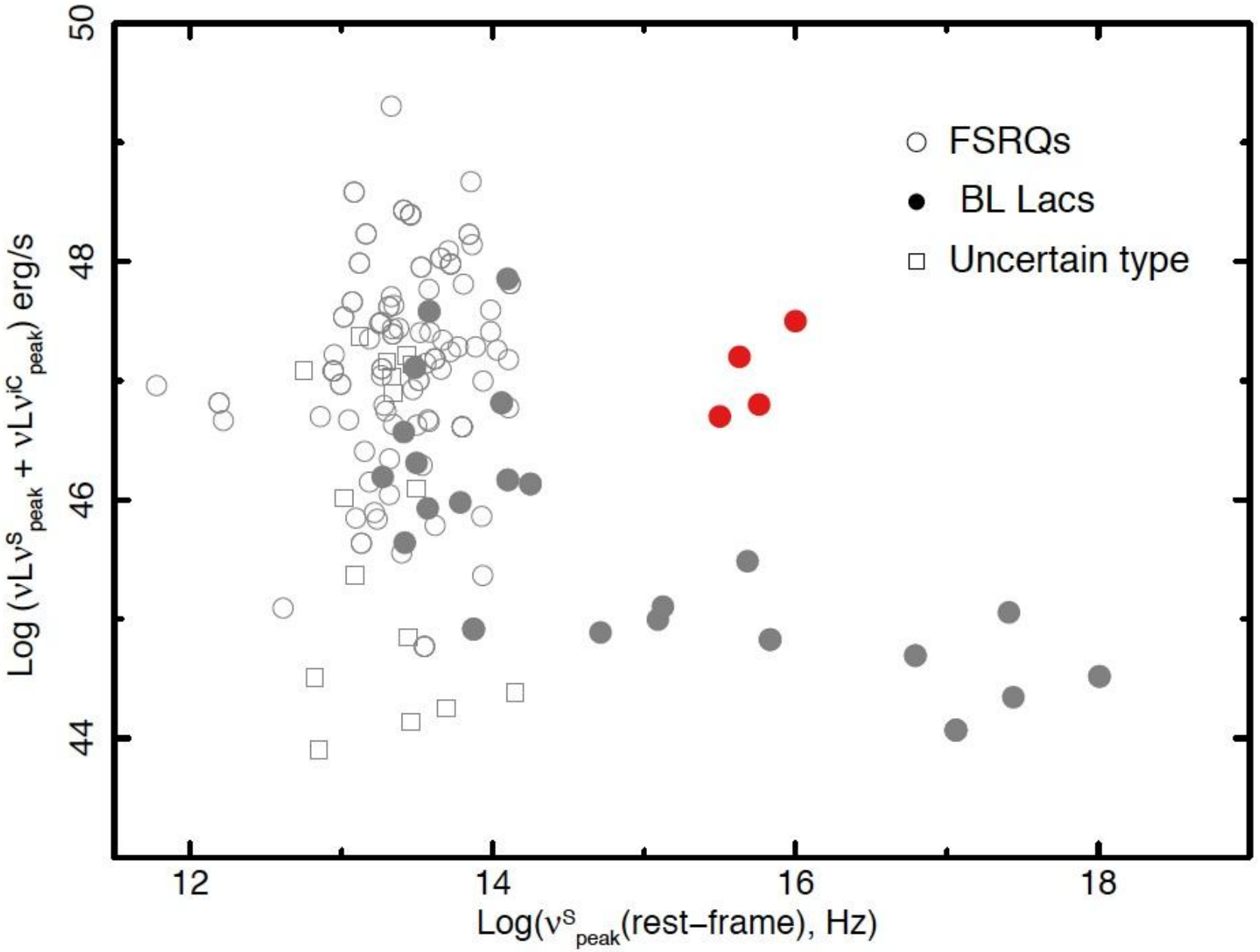
FSRQs
BL Lacs
Uncertain type
Log (νLν^S_peak + νLν^IC_peak) erg/s
Log(ν^S_peak(rest−frame), Hz)
50
48
46
44
12
14
16
18

Main conclusions

- A lot of progress has been made recently on blazar research thanks to the availability of multi-frequency data from several facilities (Planck, Swift, Fermi, TeV/Cherenkov telescopes, other ground based observatories, etc.)
- The distributions of several blazar key physical parameters have been measured and correlations have been investigated.
- The Compton dominance of (radio selected) blazars peaks at values close to 1 and it extends to values as large as 100 or more.
- Selection effects play a major role in the composition of blazar samples and cause large biases in the estimation of several parameters
- Simple SSC one-zone models are not consistent with the SED of LBL blazars, but might be consistent with the SED of HSP objects
- Simulations show that *all blazar properties* can be interpreted within a *very simple scenario* where classification in different subclasses and their peculiar evolution is the result of the combination of different components and to selection effects.
- High redshift HSP objects have been discovered, these objects are “forbidden in the Blazar sequence scenario”.
- Some distant (up to ~1.6-1.8) HSP blazars detected in the 10-100 GeV band impling that many sources of this type could be detected in future VHE experiments, particularly the CTA.